CONTE CENTER

Washington University in St. Louis

SCHOOL OF MEDICINE

Abnormalities in Volume, Area and Thickness of the Cingulate Gyrus in Schizophrenia

Lei Wang[1]; Joshua C. Trein[1]; Mokhtar H. Gado[2]; Malini Hosakere[3]; J. Tilak Ratnanather[3]; Michael I. Miller[3]; John G. Csernansky[1]

Departments of Psychiatry[1], Radiology[2], Washington University School of Medicine, St. Louis MO, and the Center for Imaging Science[3], Johns Hopkins University, Baltimore, MD, Supported by R01 MH56584, P50 MH71616 56429, P41 RR15241

Introduction

The cingulate gyrus has attracted considerable interest because of its role in deleted cognitive functions that appear to be critical for understanding schizophrenia and other neuropsychiatric disorders. In particular, the cingulate gyrus has many connections with other cortical and subcortical brain regions and plays a central role in attention and memory. Further, abnormalities in structure and function of the cingulate gyrus have been reported in subjects with schizophrenia. For example, enlarged ventricles neighboring the cingulate gyrus as well as reduced volume of the cingulate gyrus have been reported in schizophrenia subjects.

Automated methods for neuroanatomical analysis are now being developed within the field of Computational Anatomy, with particular emphasis on the analysis of the macroscopic features of the neocortical surface. The following two objectives are central to our methods for cortical analysis:

i. the construction of the 3D neocortical mantle representing the positions of the gray matter connected voxels that form the highly convoluted structure, and
ii. the construction of a triangulated graph representing the 2D submanifold of relevant surfaces (e.g. the gray/white matter boundary).

The two objectives are linked in that the 2D submanifold, and therefore its convoluted geometry, is determined by the variation, position, and density of the cortical mantle cells, manifested as gray matter at the macroscopic scale of current MRI imaging methods.

Gray matter volume is necessarily the product of the surface area of the structure and its thickness. The separate measurement of surface area and thickness, especially within small subregions that are topographically distinct, may be essential when attempting to detect subtle aberrations of neuronal cytoarchitecture. Here we describe refined applications of Bayesian segmentation, isosurface reconstruction and dynamic programming to analyze the cingulate gyrus that may have different tissue characteristics.

Anatomic Definition of the Cingulate Gyrus

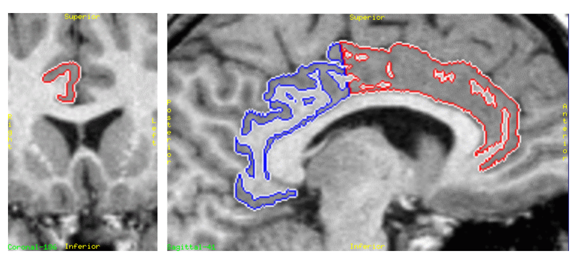

The cingulate gyrus is a curved (C-shaped) structure that surrounds and abuts the corpus callosum and lies in a position intermediate between the diencephalon and the expanded neocortex. The medial limit is the cortical surface in the interhemispheric fissure (1).

On its dorsal aspect are a number of other cortical formations, including from rostral to caudal, the superior frontal gyrus, the paracentral lobule, and the precuneus.

In coronal MR sections, the caudal end of the cingulate gyrus is the isthmus, which lies below the splenium at the most anterior limit of the calcarine sulcus. The cingulate then extends posteriorly, following the upper bank of the calcarine sulcus, until at the bifurcation point the calcarine sulcus branches into the parietooccipital fissure. At this bifurcation point, the cingulate gyrus turns upward, following the anterior bank of the subparietal sulcus. In this fashion, the cingulate gyrus wraps around the posterior limit of the splenium of the corpus callosum and is separated from the precuneus by the subparietal sulcus at the point where the cingulate sulcus is turning upward to become the marginal sulcus (cingulate sulcus marginal segment).

Moving anteriorly from this point, the cingulate sulcus separates the cingulate gyrus from the paracentral lobule and then from the superior frontal gyrus. The superior limit of the cingulate gyrus is the cortical surface forming the inferior bank of the cingulate sulcus. The inferior limit of the cingulate gyrus is the inferior surface of the cortex forming the superior bank of the callosal surface (the inferior bank being the corpus callosum). Wherever the paracingulate gyrus is present, we exclude it. As the cingulate gyrus wraps around the genu and rostrum of the corpus callosum, it tapers off gradually. The rostral end of the cingulate gyrus is defined as the most rostral coronal section through the septum pellucidum, the appearance of the paraolfactory sulcus being the delimiting landmark.

The **anterior** and **posterior** segments of the cingulate gyrus are separated by the plane bisecting the AC-PC line.

Subjects and Scans

Demographics

	N (m/f)	Age (yrs)
Schizophrenia	54 (32/22)	37.2 (±12.0)
Control	68 (35/33)	39.1 (±14.4)

MR scans

- Magnetom SP-4000 1.5-Tesla Siemens imaging system with standard head coil
- 3D Turbo-FLASH sequence (TR = 20 ms, TE = 5.4 ms, flip angle = 30°, 1 mm section thickness, 180 slices, 256-mm field of view, matrix 256 × 256, number of acquisitions = 1, scanning time = 13.5 min @ 1 × 1 × 1 mm³/voxel)

Methods

Bayesian Segmentation with Partial-Volumes

$$CSF,\ PCG,\ G,\ PGW,\ W:\ \ p(I_n \mid \mu_n(h_n), \sigma_n^2(h_n)) = \prod_{n=1}^{N} \frac{1}{\sqrt{2\pi\sigma_n^2(h_n)}}\, e^{\frac{-(I_n-\mu_n(h_n))^2}{2\sigma_n^2(h_n)}} \qquad (2).$$

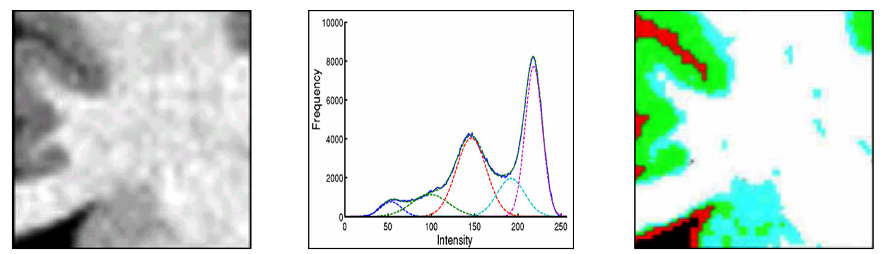

Recalibration with Neyman–Pearson Likelihood Ratio Test

$$\frac{p(I_n \mid h_n = G)}{p(I_n \mid h_n = CSF)} \underset{C}{\overset{G}{\gtrless}} \theta_{C/G},\quad \frac{p(I_n \mid h_n = W)}{p(I_n \mid h_n = G)} \underset{G}{\overset{W}{\gtrless}} \theta_{G/W} \qquad (7).$$

Topologically-Correct Isosurface

The MR subvolume is binarized according to the threshold $\theta_{G/W}$. A topology correction method is applied to the binary volume in which all handles of the WM object are removed. The original intensity of the modified voxels is then adjusted. This ensures that the binarization of the edited image is the same as the topologically correct binary image. Next, a connectivity-consistent isosurface algorithm is used to extract the isosurface of the edited image (3,4).

Cingulate Subsurface Extraction

Dynamic programming is used to define the closed-path boundaries of the sub-surface, which is assumed to be a sequence of geodesics (the shortest path between two points on the triangulated graph) (5).

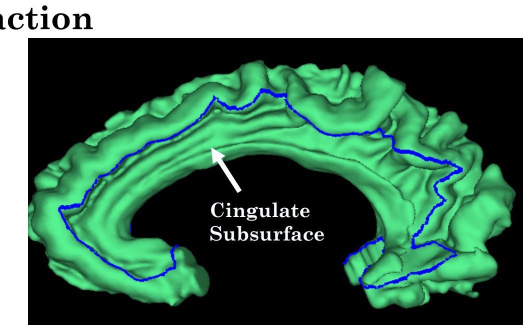

LCMDM (Labeled Cortical Mantle Distance Map)

The variation of GM-labeled voxels as a function of their position from the generated surface: A histogram of distances between the GM-labeled voxels in the segmented image and the cortical surface. For each voxel, the vertex in the triangulated surface closest to that voxel is determined, and the distance between the vertex and the voxel is measured (6).

A cumulative distribution function (CDF) of the histogram is generated for calculating surface quantities.

Results

Cortical Mantle Measures

Volume	Integration of histogram
Surface Area	Trigonometry of triangles
Cortical Mantle Thickness	Fiftieth percentile (median) of CDF

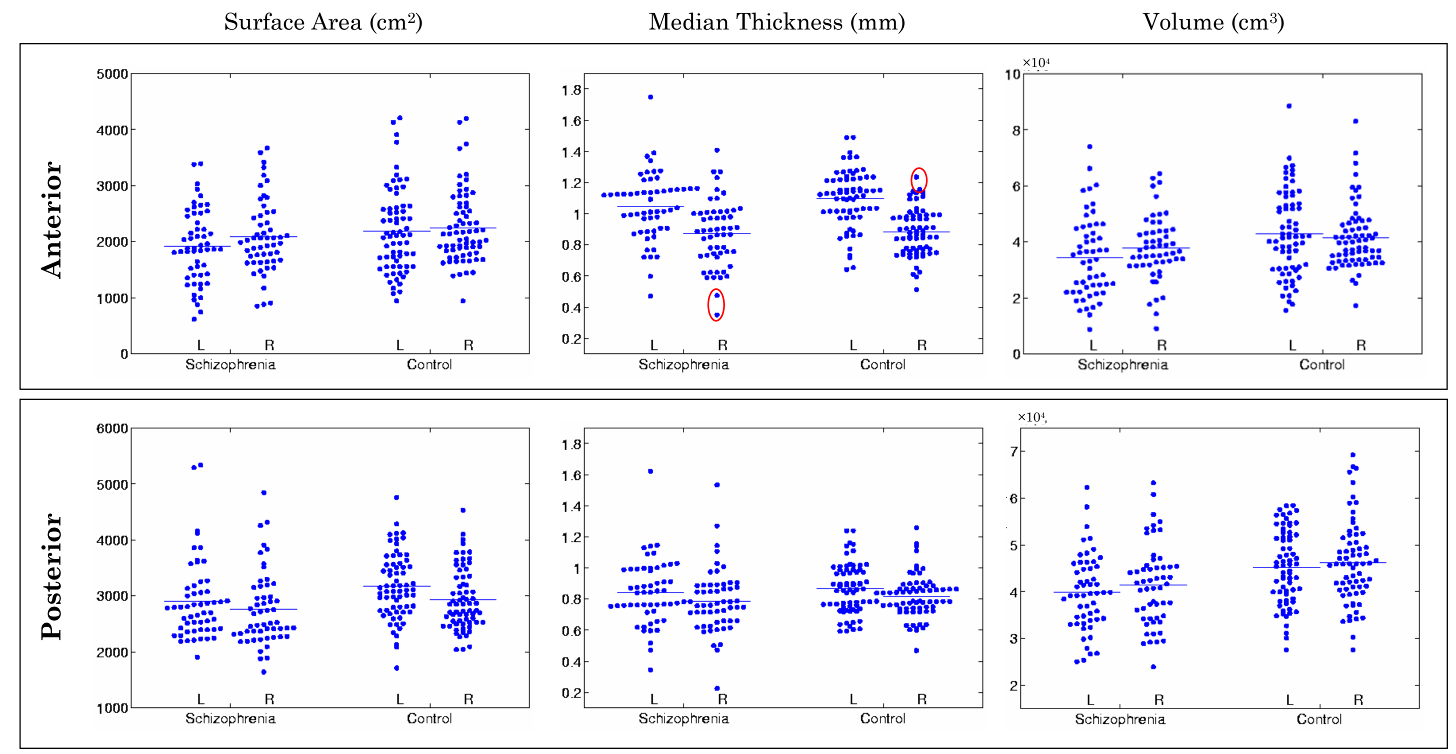

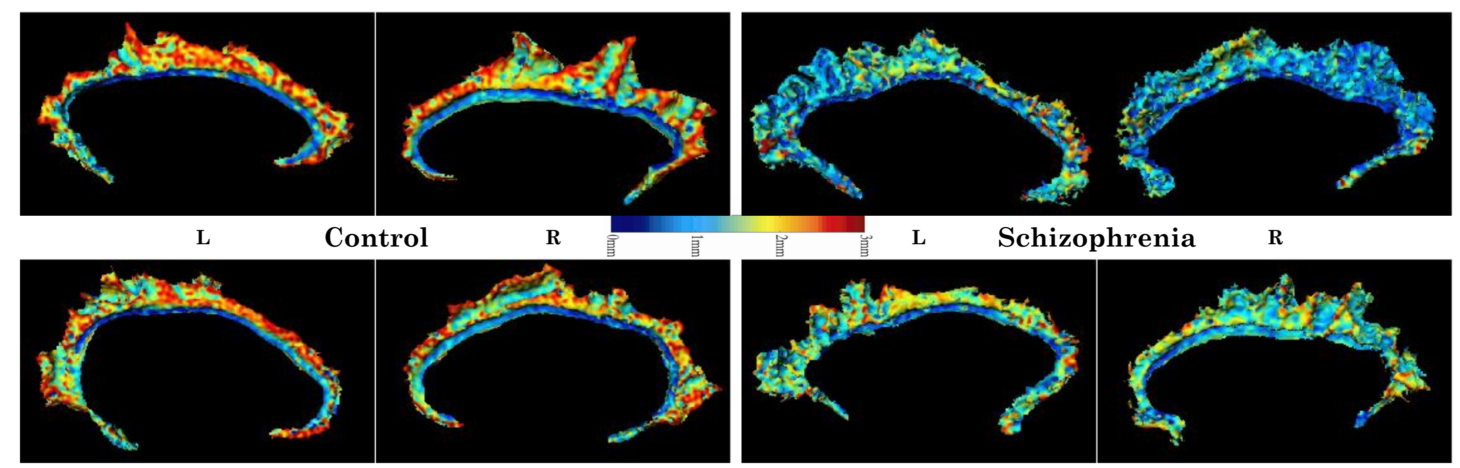

Schizophrenia vs. Control (repeated-measures ANOVA)

Anterior cingulate gyrus

• smaller volume	p = .0009
• smaller surface area	p = .046*
• smaller 50th-percentile thickness	p = .015*
• L > R: 50th-percentile thickness	p < .0001

Posterior cingulate gyrus

• smaller volume	p < .0001
• trend toward a smaller surface area	p = .085*
• smaller 50th-percentile thickness	p = .026*
• L > R: surface area	p = .0085
• L > R: 50th-percentile thickness	p = .029

*one-tailed least-square means

References

1. Duvernoy, HM., The Human Brain: Surface, Three-Dimensional Anatomy and MRI. 1991, Wien, New York: Springer-Verlag.
2. Joshi, M, et al., Brain segmentation and the generation of cortical surfaces. NeuroImage, 1999. **9**(5): p. 461-76.
3. Han, X, et al, Topology Correction in Brain Cortex Segmentation Using a Multiscale, Graph-based Algorithm. IEEE Trans. Med. Imag., 2002. **21**: p. 109-121.
4. Han, X, et al, A Topology Preserving Deformable Model Using Level Set. CVPR'2001, vol. 2. IEEE, Kauai, HI, 2001. p. 765-770.
5. Khaneja, N, et al, Dynamic programming generation of curves on brain surfaces. IEEE Trans. Pattern Anal. Mach. Intell. 1998. **20**: p.1260-1265.
6. Miller, MI, et al., Bayesian construction of geometrically based cortical thickness metrics. NeuroImage, 2000. **12**(6): p. 676-87.
7. Ratnanather, JT, Wang, L, et al, Validation of Semiautomated Methods for Quantifying Cingulate Cortical Metrics in Schizophrenia. Psychiatry Research: Neuroimaging, 2004, 132: p. 53-68.